JOC Article

A New Class of Discotic Mesogens Derived from Tris(*N*-salicylideneaniline)s Existing in C_{3h} and C_s Keto-Enamine Forms

Channabasaveshwar V. Yelamaggad,* Ammathnadu S. Achalkumar, D. S. Shankar Rao, and S. Krishna Prasad

Centre for Liquid Crystal Research, Jalahalli, Bangalore, 560 013, India

yelamaggad@gmail.com

Received June 20, 2007

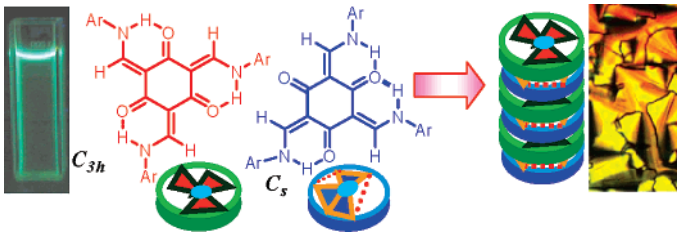

Two series of a unique class of columnar liquid crystals derived from tris(*N*-salicylideneaniline)s [TSANs] in which the proton and the electron interact with each other through the H-bonding environment are reported. The synthesis is carried out by condensing 1,3,5-triformylphloroglucinol with the respective dialkoxyanilines or trialkoxyanilines. ^{1}H NMR and ^{1}H−^{1}H COSY NMR studies revealed their existence as an inseparable mixture of two keto-enamine tautomeric forms with C_{3h} and C_s rotational symmetries instead of the expected enol-imine form. The influence of the number of peripheral alkoxy tails on the columnar mesomorphic behavior is investigated by using polarizing optical microscopy, differential scanning calorimetry, and X-ray scattering. The fluid/glassy columnar states probed for a number of representative compounds confirmed the D_{6h} (hexagonal) or D_{2h} (rectangular) symmetry of the columns. The electronic absorption and emission characteristics of these compounds have been studied in both mesomorphic and solution states. Of special interest, the photoluminescence spectra of solution and fluid/glassy two-dimensional structure evidently disclose the promising light generating capability of these new discotics systems.

Introduction

Thermally enforced self-assembly of shape-anisotropic molecules leads to the formation of liquid crystal (LC) phases wherein the molecules are mobile, yet possess orientational and/or one- or two-dimensional positional order.[1] Owing to this unique order-mobility feature, they are finding increasing applications in several important technological fields.[1e] Conventionally, the anisometric molecules employed to stabilize LC phases are either rod-like (calamitic) or disc-like (discotic). In the early 1970s,[2] the calamitics were recognized as novel materials for the display technology, and presently, they form the backbone of the flat panel display industry. The discotic LCs, discovered by Chandrasekhar et al. in 1977,[3] are becoming increasingly interesting from both scientific and application viewpoints;[4] they are slowly entering into the mainstay of organic molecular electronics. In general, disc-shaped mesogens are made of flat or nearly flat (two-dimensional) molecules

* Address correspondence to this author. Phone: 91-80-2838 1119. Fax: 91-80-28382044.

(1) (a) Chandrasekhar, S. *Liquid Crystals*, 2nd ed.; Cambridge University Press: Cambridge, UK, 1992. (b) Kato, T. *Science* **2002**, *295*, 2414−2418. (c) Tschierske, C. *Annu. Rep. Prog. Chem. Sect. C* **2001**, *97*, 191−267. (d) de Gennes, P. G.; Prost, J. *The Physics of Liquid Crystals*; Oxford Science Publication: Oxford, UK, 1993. (e) Bahadur, B. *Liquid Crystals*: *Applications and Uses*; World Scientific: Singapore, 1990; Vols. 1−3.

(2) Gray, G. W.; Harrison, K. J.; Nash, J. A. *Electron. Lett.* **1973**, *9*, 130−131.

(3) Chandasekhar, S.; Sadashiva, B. K.; Suresh, K. A. *Pramana* **1977**, *9*, 471−480.

(4) (a) Bushby, R. J.; Lozman, O. R. *Curr. Opin. Collidal Interface Sci.* **2002**, *7*, 343−354. (b) Kumar, S. *Liq. Cryst.* **2004**, *31*, 1037−1059. (c) Kumar, S. *Chem. Soc. Rev.* **2006**, *35*, 83−109. (d) Warman; J. M; Van De Craats, A. M. *Mol. Cryst. Liq. Cryst*. **2003**, *396*, 41−72. (e) Van De Craats, A. M.; Warman, J. M.; Fechtenkotter, A.; Brand, J. D.; Harbison, M. A.; Mullen, K. *Adv. Mater*. **1999**, *11*, 1469−1472.

10.1021/jo0712650 CCC: $37.00
Published on Web 10/04/2007

SCHEME 1 [a]

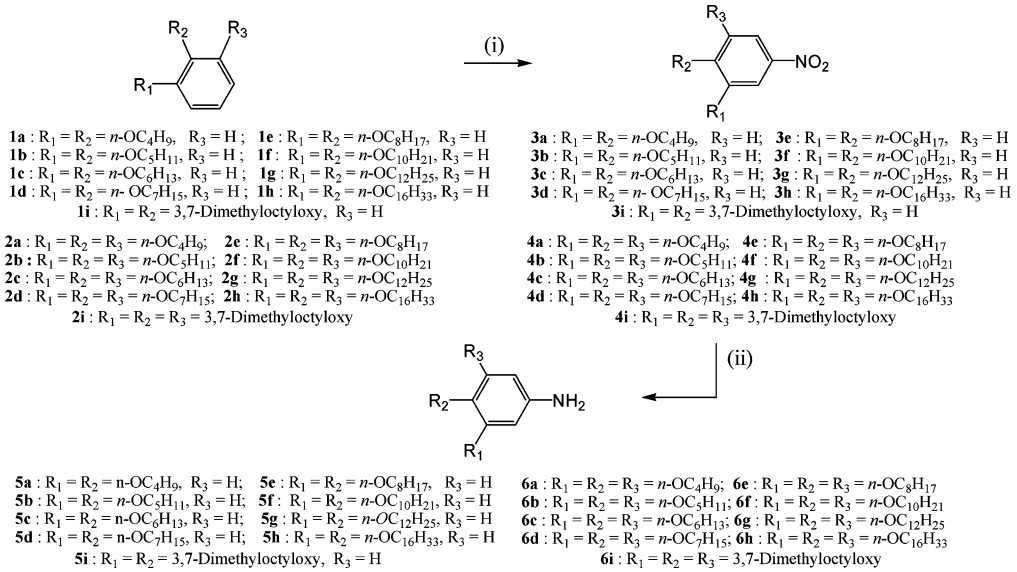

[a] Reagents and conditions: (i) 70% HNO_3, $NaNO_2$, CH_2Cl_2, rt, 1 h (50−60%); (ii) H_2 (1 atm, balloon), 10% Pd/C, THF, rt, 12 h (85−94%).

SCHEME 2 [a]

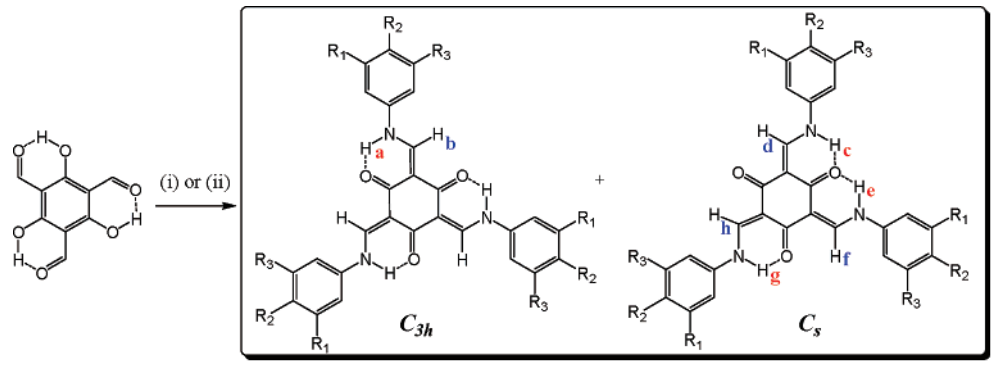

DT-n Series (C_{3h}:C_s)[b]	TT-n Series (C_{3h}:C_s)[b]
DT-4 : $R_1 = R_2 = n$-OC_4H_9, R_3 = H (1:1.99)	**TT-4** : $R_1 = R_2 = R_3 = n$-OC_4H_9 (1:0.28)
DT-5 : $R_1 = R_2 = n$-OC_5H_{11}, R_3 = H (1:2.43)	**TT-5** : $R_1 = R_2 = R_3 = n$-OC_5H_{11} (1:1.07)
DT-6 : $R_1 = R_2 = n$-OC_6H_{13}, R_3 = H (1:2.47)	**TT-6** : $R_1 = R_2 = R_3 = n$-OC_6H_{13} (1:1.98)
DT-7 : $R_1 = R_2 = n$-OC_7H_{15}, R_3 = H (1:2.48)	**TT-7** : $R_1 = R_2 = R_3 = n$-OC_7H_{15} (1:2.97)
DT-8 : $R_1 = R_2 = n$-OC_8H_{17}, R_3 = H (1:1.8)	**TT-8** : $R_1 = R_2 = R_3 = n$-OC_8H_{17} (1:1.09)
DT-10 : $R_1 = R_2 = n$-$OC_{10}H_{21}$, R_3 = H (1:1.87)	**TT-10** : $R_1 = R_2 = R_3 = n$-$OC_{10}H_{21}$ (1:1.08)
DT-12 : $R_1 = R_2 = n$-$OC_{12}H_{25}$, R_3 = H (1:2.21)	**TT-12** : $R_1 = R_2 = R_3 = n$-$OC_{12}H_{25}$ (1:0.95)
DT-16 : $R_1 = R_2 = n$-$OC_{16}H_{33}$, R_3 = H (1:2.2)	**TT-16** : $R_1 = R_2 = R_3 = n$-$OC_{16}H_{33}$ (1:1.23)
DT-8B: $R_1 = R_2$ =3,7-Dimethyloctyloxy, R_3 = H (1:1.3)	**TT-8B**: $R_1 = R_2 = R_3$ = 3,7-Dimethyloctyloxy (1:1.2)

[a] Reagents and conditions: (i) **5a**−**i**, ethanol, reflux, 6 h (60−75%); (ii) **6a**−**i**, ethanol, reflux, 6 h (65−87%). [b]The ratio of C_{3h} and C_s isomers was determined by comparing the integral areas of amine protons H_a (C_{3h} isomer) vs H_c, H_e, and H_g (C_s isomer) in ^{1}H NMR.

having[4] 3-, 4-, or 6-fold rotational symmetry, to which are attached, via ester, or ether, or thioether links, several alkyl chains of the same or even different lengths. Owing to the attractive interactions between similar molecular fragments, i.e., aromatic cores and flexible paraffinic tails, an effective nanosegregation occurs among them, and thus the columnar phase is preferred over the nematic (N) phase. The Col phases, characterized by indefinitely long molecular columns, aggregating into two-dimensional (2D) lattices with different symmetries, are of great significance. This is because these one-dimensional (1D) Col stacks facilitate smooth charge-transport (as high as 1.0 $cm^2\ V^{-1}\ S^{-1}$) along the column axis[4] that can be initiated either by making a charge transfer (CT) complex or by photolysis. In addition, they offer the possibility of combining several physical properties with the orientational control of the molecular order, self-healing of structural defects, and the ease of processability when compared with inorganic semiconductors or zone refined single crystals or conductive polymers used in electronic applications.[5] Thus, the anisotropy in electrical conduction of fluid Col phase can be well exploited in molecular electronic devices such as one-dimensional conductors,[6] photoconductors,[7] molecular wires and fibers,[8] organic light emitting diodes (OLEDs),[9] field-effect transistors, and photovoltaic

(5) (a) Heeger, A. J. *Angew. Chem., Int. Ed.* **2001**, *40*, 2591−2611. (b) Kertesz, M.; Choi, C. H.; Yang, S. J. *Chem. Rev.* **2005**, *105*, 3448−3481. (c) Pope, M.; Swenberg, C. E. *Electronic Processes in Organic crystals and Polymers*; Oxford University Press; Oxford, UK, 1999. (d) Mullen, K.; Wenger, G. *Electronic Materials*: *The Oliogomer Appraoch*; Wiley-VCH: New York, 1998. (e) McQuade, D. T.; Pullen, A. E.; Swager, T. M. *Chem. Rev.* **2000**, *100*, 2537−2574.

TABLE 1. Phase Transition Temperatures[a] (°C) and Corresponding Enthalpies (kJ/mol) of the DT-*n* Series[f]

compd **DT-*n***	phase sequence: heating	phase sequence: cooling
DT-4	Cr 128.5 [39.2] I	I 104 [30.7] Cr
DT-5	Cr 104 [5.6][b] Col_h 119.3 [3.3] I	I 117 [3.3] Col_h 57.3 [1.4] Cr
DT-6	Cr 84.9 [32.6][b] Col_r 131.7 [3.6] I	I 129.8 [4] Col_r[c,d]
DT-7	Cr 75.3 [24.7] Col_r 138 [4.2] I	I 136.3 [4.1] Col_r[c,d]
DT-8	Cr 75.6 [39.8] Col_r 136.4 [5.3] I	I 135 [5.2] Col_r 57 [1.1] X[e]
DT-10	Cr 82.6 [49] Col_r 141.9 [5.2] I	I 140.9 [5.8] Col_r[c,d]
DT-12	Cr 82.6 [77.1] Col_r 133.9 [7.1] I	I 132.7 [6.5] Col_r[c,d]
DT-16	Cr 73.4 [53.9] Col_r 127.3 [7.1] I	I 126.2 [6.9] Col_r 51.5 [62.9] Cr
DT-8B	Col_h 109.9 [2.7] I	I 105.5 [2.6] Col_h[c]

[a] Peak temperatures in the DSC thermograms obtained during the first heating and cooling cycles at a rate of 5 deg/min. [b] **DT-5** and **DT-6** show additional Cr-to-Cr transitions during the first heating cycle at 96.5 [24.2] and 65.5 [1.1], respectively. [c] In DSC thermogram(s) of first/subsequent cooling cycle(s), no other signatures were found until −60 °C; similarly, in microscopic observation the texture of the Col phase remains unaltered until room temperature (30 °C). [d] The Col phase loses its fluidity below ∼60 °C as it perhaps freezes into a glassy state. [e] This phase supercools until −60 °C. [f] Cr = crystal; Col_h = hexagonal columnar phase; Col_r = rectangular columnar phase; I = isotropic liquid; X = perhaps a glass.

cells.[10] The performance of such electronic devices critically depends on the high charge-carrier mobility. Consequently, there have been intensive investigations to find discotics with the Col phase at room temperature or Col glasses possessing high charge mobility.

Recently, based on the work of MacLachalan et al.,[11] we have discovered that an altogether new class of disc-like organic molecules derived from tris(*N*-salicylideneanilines) [TSANs], existing in an inseparable mixture of two keto-enamine forms with C_{3h} and C_s rotational symmetries, display Col phase(s) solely.[12] These discogens are rather unique: First, because the central core of these systems, which is the size of polyaromatics, is a flat electron-accepting (*n*-type) entity featuring multiple strong intramolecular hydrogen (H) bonding between the 2°-amine protons and oxygens of the cyclohexanetrione. Second, the individual column is resulting from the self-assembly of a mixture of two geometrical isomers (having C_{3h} and C_s symmetry in varying proportions) in close (core−core) spatial proximity. Third, owing to the possibility of contiguous three-proton transfer and a simultaneous rearrangement of the π-orbitals in these systems, a coupling between motions of the proton and the conduction electron might be produced, which is a key phenomenon for many proposed molecular electronic devices. Furthermore, in a later study, we noted that these materials possess some promising electronic (inherent fluorescence) property due to extended π-conjugations.[12b] In this context, there have been several recent innovations where the electronic properties of TSANs, in particular the C_{3h} isomer, can be effectively altered by changing the peripheral substitutions. For example, Lee and co-workers have determined that stereoelectronic control of self-assembly of C_{3h} isomers can enhance their fluorescence efficiency in solutions.[13a] Subsequently, it was also shown that by manipulating a mutually reinforcing H-bond network in the C_{3h} isomer, a 2D conjugated system with fast and reversible conformational switching, and thus fluorescence switching, can be obtained.[13b] These results are quite significant given the fact that the beneficial self-organizing nature of discotics into large and well-organized

TABLE 2. The Results of Indexation of XRD Profiles at a Given Temperature (*T*) of Phases Displayed by the Compounds of the DT-*n* Series

compd	*T* (°C)	phase	*d* (Å) measd	*d* (Å) calcd	Miller index *hkl*	lattice parameters (Å)
DT-5	90	Col_h	22.7	22.6	100	$a = 26.1$
			13.1	13.1	110	$c = 3.32$
			11.3	11.3	200	
			8.5	8.6	210	
			7.5	7.6	300	
			6.8	6.6	220	
			6.5	6.6	220	
			4.5			
			3.32		001	
DT-8	70	Col_r	27.0	27.1	110	$a = 41.5$
			20.8	20.8	200	$b = 35.7$
			13.5	13.5	220	$c = 3.3$
			7.8	7.8	430	
			7.4	7.5	340	
			6.7	6.8	250	
			6.2	6	060	
			4.5			
			3.3		001	
	30	X	27.1	27.1	110	$a = 39.7$
			19.9	19.9	200	$b = 37.1$
			13.5	13.8	220	$c = 3.26$
			7.7	7.6	430	
			7.4	7.6	050	
			6.7	6.9	530	
			6.2	6.0	060	
			4.4			
			3.26		001	
DT-8B	90	Col_h	26.1	26.1	100	$a = 30.1$
			4.9			$c = 3.5$
			3.5		001	
	22	Col_h	27.0	27	100	$a = 31.2$
			4.8			$c = 3.39$
			3.39		001	

(6) (a) Adam, D.; Schuhamcher, P.; Simmerer, J.; Haussling, L.; Siemensmeyer, K.; Etzbach, K. H.; Ringsdorf, H.; Haarer, D. *Nature* **1994**, *371*, 141−143. (b) Fontes, E.; Heiney, P. A.; De Ju, W. H. *Phys. Rev. Lett.* **1988**, *61*, 1202−1205.

(7) Chandrasekhar, S.; Balagurusamy, V. S. K. *Proc. R. Soc. London, Ser. A* **2002**, *458*, 1783−1794.

(8) (a) Osburn, E. J.; Schmidt, A.; Chau, L. K.; Chen, S. Y.; Smolenyak, P.; Armstrong, N. R.; O'Brian, D. F. *Adv. Mater.* **1996**, *8*, 926−928. (b) Percec, V.; Glodde, M.; Bera, T. K.; Miura, Y.; Shiyanovskaya, I.; Singer, K. D.; Balagurusamy, V. S. K.; Heiney, P. A.; Schnell, I.; Rapp, A.; Spiess, H.-W.; Hudsonk, S. D.; Duank, H. *Nature* **2002**, *419*, 384−387.

(9) Christ, T.; Glusen, B.; Greiner, A.; Kettner, A.; Sander, R.; Stumpflen, V.; Tsukruk, V.; Wendorff, D. J. *Adv. Mater.* **1997**, *9*, 48−52.

(10) Schmidt-Mende, L.; Fechtenkotter, A.; Mullen, K.; Moons, E.; Friend, R. H.; MacKenzie, J. D. *Science* **2001**, *293*, 1119−1126.

(11) Chong, J. H.; Sauer, M.; Patrick, B. O.; MacLachlan, M. J. *Org. Lett.* **2003**, *21*, 3823−3826.

(12) (a) Yelamaggad, C. V.; Achalkumar, A. S.; Rao, D. S. S.; Prasad, S. K. *J. Am. Chem. Soc.* **2004**, *126*, 6506−6507. (b) Yelamaggad, C. V.; Achalkumar, A. S. *Tetrahedron Lett.* **2006**, *47*, 7071−7075.

(13) (a) Riddle, J. A.; Lathrop, S. P.; Bollinger, J. C.; Lee, D. *J. Am. Chem. Soc.* **2006**, *128*, 10986−10987. (b) Jiang, X.; Bollinger, J. C.; Lee, D. *J. Am. Chem. Soc.* **2006**, *128*, 11732−11733.

domains has been shown to improve the OLED characteristics. However, the vast majority of discotics cannot be used as the active emissive layer in OLEDs owing to their low luminescence efficiency. This has led to many attempts to design the intrinsically luminescent disc-like mesogens, which self-assemble to form the fluid Col structure with oriented luminophores.[14] In this respect, the Col phase derived from TSANs should further benefit from emission efficiency due to its intrinsic 2D π-conjugation wherein the central cyclohexane-1,3,5-trione is electron deficient while the peripheral aromatic cores bearing multiple alkoxy tails are electron donating. In addition, TSANs have proved promising in fabricating novel molecular materials. MacLachlan et al.[15a] have revealed that upon appending with additional functional groups, TSANs may form H-bonded capsules, clefts, and chains while Riddle and co-workers[15b] have shown that sterically hindered TSANs could be used as mechanically coupled biconcave molecules, which can release the clatherated guest molecules.

In essence, the aforementioned studies clearly imply that TSANs have a truly versatile molecular architecture in which both electronic as well as novel molecular material features (self-organizing ability, fluidity, molecular recognition, etc.) can be imbued. Nonetheless, to reveal their in-depth and/or other physicochemical properties, elaborative synthetic studies are essential. In this direction, the understanding of their mesomorphic behavior, as mentioned earlier, is at a rather primitive stage.[12] Seeking an elaborative study, a large number of TSANs have been obtained; here we present the first detailed investigation on the synthesis, molecular structural characterization, phase behavior, and photophysical properties of two series of TSANs differing in their peripheral aromatic core substitutions. These two sets of TSANs possessing two and three alkoxy tails on each of the three benzene rings linked to the central cyclohexane-1,3,5-trione have been abbreviated as the **DT-*n*** series and the **TT-*n*** series, respectively, where **DT** and **TT** refer to **D**ialkoxy-**T**SANs and **T**rialkoxy-**T**SANs, respectively, while ***n*** indicates the number of carbon atoms in the alkoxy chains.

Results and Discussion

Synthesis and Molecular Structural Characterization. The reaction sequences adopted to prepare the intermediates and the target **DT-*n*** and **TT-*n*** series of compounds are depicted in Schemes 1and 2, respectively. As shown in Scheme 1, 1,2-dialkoxybenzenes (**1a**−**i**) and 1,2,3-trialkoxybenzenes (**2a**−**i**)[16] were subjected to the two-phase nitration[17a] by using an aqueous solution of nitric acid (70%) and sodium nitrite in dichloromethane to achieve the corresponding 3,4-dialkoxynitrobenzenes (**3a**−**i**) and 3,4,5-trialkoxynitrobenzenes (**4a**−**i**). The catalytic ($Pd-C/H_2$) hydrogenation of these nitro derivatives furnished the key 3,4-dialkoxyanilines (**5a**−**i**) and 3,4,5-trialkoxyanlines (**6a**−**i**)[17b] in almost quantitative yields. Finally, as shown in Scheme 2, the condensation reaction between 1,3,5-triformylphloroglucinol[11,12] and 4 equiv of alkoxyanilines **5a**−**i** and **6a**−**i** in refluxing ethanol afforded the requisite **DT-*n*** and **TT-*n*** series of discotics, respectively, in reasonably good yields. The spectroscopic data as well as the results of elemental analyses were found to be consistent with the proposed molecular structure of all the intermediates and final compounds. The ^{1}H NMR spectra of both the **DT-*n*** and **TT-*n*** series of discotic TSANs showed the expected complex pattern in the downfield region and thus evidenced their occurrence as a mixture of the above-mentioned two keto-enamine tautomeric forms. (See the experimental procedures section as well as the Supporting Information for details.)

Mesomorphic Behavior. The phase behavior of the synthesized TSANs was established with the aid of a polarizing optical microscope (POM), a differential scanning calorimeter (DSC), and X-ray diffraction (XRD). A sample placed between a clean untreated glass slide and a cover slip was used for the POM study. The preliminary mesophase assignment was based on the two inherent properties displayed by mesogenic TSANs: the birefringence and fluidity. The signatures observed in DSC thermograms due to phase transitions of all the samples were consistent with those of the optical experiments. In general, the phase transition temperatures deduced from calorimetric measurements of the first heating and cooling cycles at a rate of 5 deg/min are presented. However, when the thermal signatures were not observed in DSC thermograms, the transition temperatures have been taken from the microscopic observations. It is important to mention here that the phase transitions and their temperatures in both optical and calorimetric studies are highly reproducible for any number of heating/cooling runs demonstrating that TSANs possess excellent thermal stability. The details of these investigations with analysis of the results of both series of compounds are presented in the sections to follow.

DT-*n* Series. The phase sequence, transition temperatures, and associated enthalpies of TSANs with two exterior alkoxy tails on each benzene ring belonging to the **DT-*n*** series are summarized in Table 1. As can be seen, all but one of the homologues are liquid crystalline; the first member **DT-4** with *n*-butyloxy tails does not exhibit mesomorphism implying that the peripheral chain melting (disordering) temperature is higher than the temperature at which stacking of the TSAN cores becomes unfavorable.[18] In other words, the chain length is not enough to increase the disorder at the periphery of the molecule to stabilize the mesophase. Other members of the series exhibit enantiotropic monomesomorphic behavior, in particular, the Col phase that was preliminarily characterized by the optical textures.

On cooling from the isotropic liquid, all the LC TSANs, except **DT-8B** (as we shall discuss later), displayed a striking fan-like growth pattern that eventually coalesces to a mosaic texture with interspersed bright and dark areas as shown in Figure 1, panels a and b. This texture remains unaltered until room temperature for TSANs **DT-6**, **DT-7**, **DT-8**, **DT-10**, and **DT-12**, although the phase could not be mechanically sheared

(14) (a) Ecoffet, C.; Markovitsi, D.; Jallabert, C.; Strzelecka, H.; Veber, M. *Thin Solid Films* **1994**, *242*, 83−87. (b) Marguet, S.; Markovitsi, D.; Goldmann, D.; Janietz, D.; Praefcke, K.; Singer, D. *J. Chem. Soc., Faraday Trans.* **1997**, *93*, 147−155. (c) Cormier, R. A.; Gregg, B. A. *Chem. Mater.* **1998**, *10*, 1309−1319. (d) Rohr, U.; Schlichting, P.; Bohm, A.; Gross, M.; Meerholz, K.; Brauchle, C.; Mullen, K. *Angew. Chem., Int. Ed.* **1998**, *37*, 1434−1437. (e) Ito, S.; Herwig, P. T.; Bohme, T.; Rabe, J. P.; Rettig, W.; Mullen, K. *J. Am. Chem. Soc.* **2000**, *122*, 7698−7706. (f) Benning, S. A.; Hassheider, T.; Keuker-Bauman, S.; Bock, H.; Salla, F. D.; Frauenheim, T.; Kitzerow, H. S. *Liq. Cryst.* **2001**, *28*, 1105−1113. (g) Attias, A. J.; Cavalli, C.; Donnio, B.; Guillon, D.; Hapiot, P.; Malthete, J. *Chem. Mater.* **2002**, *14*, 375−384.

(15) (a) Sauer, M.; Yeung, C.; Chong, J. H.; Patrick, B. O.; MacLachlan, M. J. *J. Org. Chem.* **2006**, *71*, 775−788. (b) Riddle, J. A.; Bollinger, J. C.; Lee, D. *Angew. Chem. Int. Ed.* **2005**, *44*, 6689−6693.

(16) See the Supporting Information.

(17) (a) Zinsou, A.; Veber, M.; Strzelecka, H.; Jallabert, C.; Fourre, P. *New J. Chem.* **1993**, *17*, 309−313. (b) Percec, V.; Schlueter, D.; Ronda, J. C.; Johansson, G. *Macromolecules* **1996**, *29*, 1464−1472.

(18) Collard, D. M; Lillya, C. P. *J. Am. Chem. Soc.* **1991**, *113*, 8577−8583.

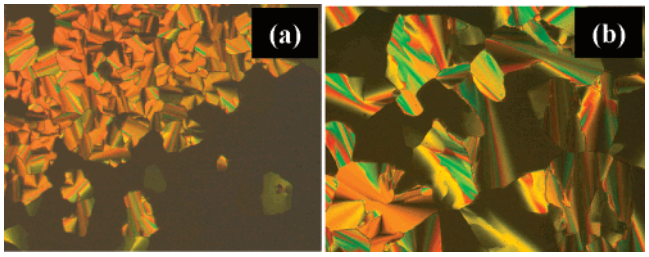

FIGURE 1. Photomicrographs of the textures observed for the Col phase of **DT-5** at 69 °C (a) and **DT-12** at 119 °C (b).

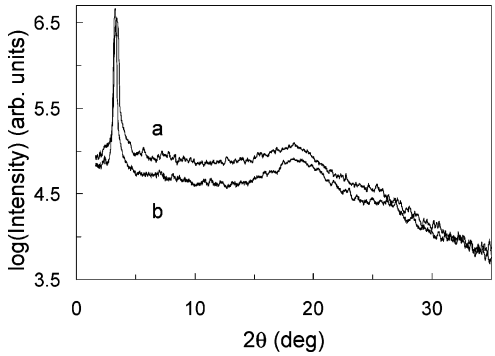

FIGURE 2. Intensity vs 2θ profile derived from the 2D XRD pattern of the Col_h phase at 90 (a) and 22 °C (b) for compound **DT-8B**.

below ~60 °C. The DSC thermograms of these TSANs obtained during the first cooling or second heating cycles, except for **DT-8**, show only a peak due to I-Col or Col-I transition, respectively. On the other hand, the thermograms of the first cooling (till − 60 °C) and second heating (from −60 °C) cycles of TSAN **DT-8**[16] possessed additional signatures at 57 (ΔH = 1.1 kJ/mol) and 72 °C (ΔH = 1.1 J/g), respectively, that can be ascribed to a transition from the Col phase to an immobile phase (hereafter referred to as X). In the optical study, no textural change was seen across the Col-X phase transition. However, as we shall see later, the XRD study revealed that the X phase possesses the features of a Col structure having a rectangular symmetry. Apparently, both optical and calorimetric studies suggest that TSANs **DT-6**, **DT-7, DT-8, DT-10**, and **DT-12** form the glassy Col phase at room temperature; this behavior is notable given the fact that such a two-dimensional (2D) structure enables the charge migration with the concomitant freezing of ionic impurities.[8b]

The general observation that discotics exhibit two main types of Col phases with D_{6h} (hexagonal) and D_{2h} (rectangular) symmetries, the phases of TSANs **DT-5** and **DT-8**, as representative cases was probed with the help of powder XRD experiments. The results of indexing the powder pattern of the phase(s) are summarized in Table 2. The low-angle region ($0 < 2\theta < 5$ °) of the diffractogram obtained[16] for the Col phase of **DT-5** at 90 °C displays a strong reflection corresponding to a Bragg spacing (d) of 22.7 Å in addition to a set of weak reflections: the five low-angle sharp maxima with the ratio of their reciprocal spacings being $1:\sqrt{3}:\sqrt{4}:\sqrt{7}:\sqrt{9}$ (within experimental limits). These are indexed to (100), (110), (200), (210), and (300) reflections of a quasi-2D hexagonal lattice with a spacing of about 26 Å. In the wide-angle region of the diffractogram two broad reflections were observed indicating that the ordering within the columns is not long-range. The first peak corresponding to a distance of 4.5 Å is diagnostic of the liquid-like disorder of the chains, while the relatively sharp but still diffuse second reflection corresponding to a distance of 3.32 Å arises due to the stacking of the TSAN cores within a column. Thus, the X-ray data in conjunction with the textural pattern suggest that the mesophase is indeed the hexagonal columnar (Col_h) phase. Interestingly, the XRD patterns obtained for the fluid Col (at 70 °C) and immobile X (at 30 °C) phases of compound **DT-8** were found to be qualitatively identical. They showed several sharp Bragg peaks in the low-angle region besides two broad reflections at wide angles corresponding to the distances in the range of ~4.5 to ~3.3 Å that relates to the liquid-like order of the peripheral tails and the stacking distance of TSANs within the same column, respectively. The first three sharp reflections of Col and X are in the ratio of 1:0.76:0.5 and 1:0.73:0.5, respectively, and can be assigned to (110), (200), and (220) reflections from a rectangular lattice. Thus, the higher temperature fluid phase is a rectangular Col (Col_r) phase, while this structure seems to be frozen in the X phase. Importantly, the core−core separation value, viz. 3.26 Å of the frozen Col structure, is near the lowest values observed for a Col phase with high charge carrier ability reported for the case of a complex with two phthalocyanine cores linked by a lutetium atom.[19] It is important to mention here that the core−core stacking in a Col structure bears a great significance because this is dependent on the magnitude of correlations between the cores, which in turn is dependent on the size of the core. Such a correlation peak is not observed for the benzene hexanoates,[20] where the core size is smaller, whereas for the triphenylene (having a larger core) systems it is commonly observed. Therefore, it is likely that strong intramolecular H-bonding leads to the formation of an effective larger core of TSAN, which could be considered as a close structural surrogate to aromatic cores (see a later section for details).

Interestingly, TSAN **DT-8B**, with peripheral branched alkoxy chains, displayed the Col phase over a wide thermal interval (~160 °C) well below and above room temperature as established by several complementary techniques, described below. In fact, the initiative of synthesizing the TSAN **DT-8B** molecule and its trialkoxy analogue **TT-8B** (see later section for details) was based on the widespread theme that when branched alkyl chains are introduced at the peripheral region of discotic molecules, the liquid-like disorder is enhanced. In particular, branched alkyl chains facilitate the widening of the mesophase thermal range and lowering of melting points without altering the type of the mesophase.[21] Compound **DT-8B**, placed between an ordinary glass slide and cover slip, could be readily spread around the slide at room temperature by mechanical shearing. The spread-over samples showed a highly birefringent texture, clearly indicating that the compound is already in the LC state. On cooling at a rate of 5 deg/min from their isotropic (I) phase, it showed a mesophase at 105 °C. Notably, the optical texture remains unchanged until room temperature and no sign of crystallization was noticed even after maintaining the samples at low temperature or even when sheared. The DSC thermograms obtained during the several heating and cooling scans corroborated the microscopic observations and further supported

(19) Van de Crats, A. M.; Warman, J. M.; Hasebe. H.; Naito, R.; Ohta, K. *J. Phys. Chem. B* **1997**, *101*, 9224−9232.

(20) Safinya, C. R.; Clark, N. A.; Liang, K. S.; Varady, W. A.; Chiang, L. Y. *Mol. Cryst. Liq. Cryst.* **1985**, *123*, 205−216.

(21) (a) Schouten, P. G.; Warman, J. H.; de Haas, M. P.; van Nostrum, C. F.; Gelinck, G. G.; Nolte, R. J. M.; Copyn, M. J.; Zwikker, J. W.; Engel, M. K.; Hanack, M.; Chang, Y. H.; Ford, W. T. *J. Am. Chem. Soc*. **1994**, *116*, 6880−6894. (b) Kumar, S.; Rao, D. S. S.; Prasad, S. K. *J. Mater. Chem.* **1999**, *9*, 2751−2754.

TABLE 3. Phase Transition Temperatures[a] (°C) and Corresponding Enthalpies (kJ/mol) of the TT-*n* Series

compd TT-*n*	phase sequence	
	heating	cooling
TT-4	Cr 176.1 [6.6] Col_r 219.1 [0.8] Col_h 246 [8.1] I	I 245 [7.8] Col_h 218 [0.7] Col_r 171.6 [6.6] Cr
TT-5	Cr 168.5 [1] Col_r 186.5 [0.4] Col_h 228.6 [7.9] I	I 226.7 [7.7] Col_h 185.5 [0.5] Col_r 69.7 [0.8] Cr
TT-6	Cr 55.4 [8.4] Col_r 173.4b Col_h 214.6 [10.3] I	I 210.2 [8] Col_h 171.5[b–d] Col_r
TT-7	Cr 54.2 [10.1] Col_r 156.2b Col_h 197 [10] I	I 195.3 [9.5] Col_h 154.4[b–d] Colr
TT-8	Cr 57.2 [8.3] Col_r 164.4b Col_h 186.2 [13.7] I	I 185.1 [12.7] Col_h 163[b] Col_r 56 [7.6] Cr
TT-10	Cr 64.2 [8.3] Col_r 158.5b Col_h 175.2 [14.7] I	I 173.6 [14.4] Col_h 157.7[b] Col_r 62.9 [11.2] Cr
TT-12	Cr 52.9 [50.9] Col_r 148.5b Col_h 163.5 [22.2] I	I 162.1 [15.1] Col_h 147.5[b] Col_r 44.8 [86] Cr
TT-16	Cr 59.9 [136.1] Col_r 96.9 [7.5] Col_h 128.1 [1.6] I	I 126.2 [4.4] Col_h 92.8 [8.8] Col_r 53.8 [62.3] Cr
TT-8B	Col_r 68[b] Col_h 109.9 [7.5] I	I 106.3 [38.1] Col_h 64[b,c] Col_r

[a] Peak temperatures in the DSC thermograms obtained during the first heating and cooling cycles at 5 deg/min. [b] The phase transition observed with a polarizing microscope was too weak to be detected by DSC. [c] No other phase transition was observed until −60 °C. [d] The Col phase loses its fluidity below ~60 °C as it perhaps freezes into a glassy state

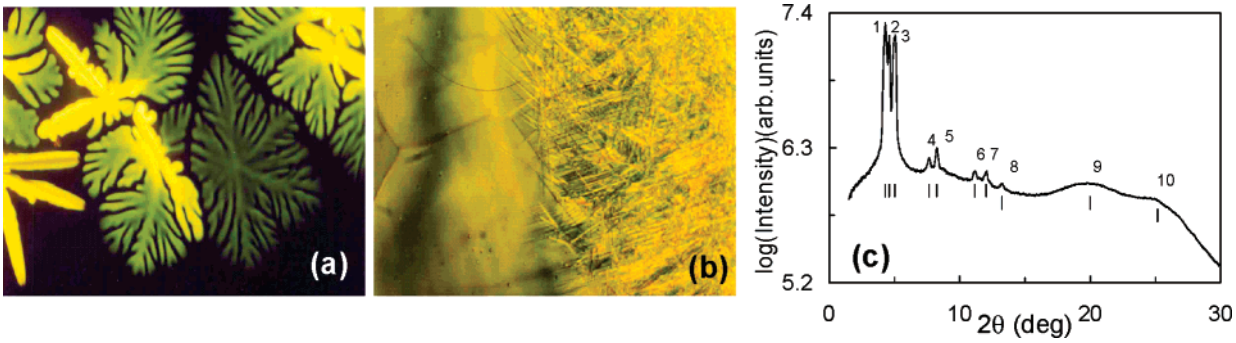

FIGURE 3. (a) Optical photomicrograph of the texture of the Col_h phase obtained for **TT-4** at 242 °C. (b) Microphotograph showing the appearance of the Col_r phase with tiny needles (see right portion) over the mosaic pattern (see left portion) of the Col_h phase of **TT-4** at 218 °C. (c) The intensity vs 2θ profile extracted from the XRD pattern of the Col_r phase of **TT-4** at 190 °C.

the repeatability of the transitions. For example, the DSC trace obtained during the first heating cycle from −60 °C showed only one endothermic peak corresponding to the Col−Iso transition.[16] In the subsequent cooling scan (down to −60 °C), as expected, a sharp exothermic peak due to an Iso−Col transition was seen. Furthermore, identical DSC profiles are obtained for the second (or any number of subsequent) heating−cooling runs. These results clearly demonstrate that the phase transitions are highly reproducible and thus TSAN **DT-8B** exhibits the Col phase over a much broader thermal range through room temperature. To elucidate the symmetry of the Col phase, powder XRD investigation was carried out at 90 °C and ambient temperature (22 °C); as expected, the diffractograms showed an identical pattern as shown in Figure 2. The wide-angle region of both high- and low-temperature profiles consisted of a diffuse reflection at 4.86 and 4.76 Å, respectively (Table 2), that can be attributed to the average distance between the liquid-like (molten) aliphatic side chains. Of special significance, a sharp Bragg (100) peak with spacing of 26.1 and 27 Å at 90 and 22 °C, respectively, was observed in the small-angle region. The absence of the expected multiple reflections in this Col phase can be ascribed to a minimum in the form factor.[22c,23] Though the occurrence of only one (100) peak precludes the unequivocal assignment of the mesophase structure, the situation is reminiscent of several reports wherein such a pattern has been assigned to a Col_h phase.[22c,23] Further, the absence of a core−core separation peak implies that the discs within a column are not well organized when compared to the normal chain analogue **DT-8**.

TT-*n* Series. Table 3 depicts the phase sequence, transition temperatures, and associated enthalpies of the **TT-*n*** series of compounds. It is seen that all the TSANs display dimesomorphic behavior involving a transition from the lower temperature Col_r to the higher temperature Col_h phase. In comparison with their dialkoxy analogues (**DT-*n*** series), these TSANs having three alkoxy chains on each benzene ring, except a few, show lower melting (Cr-Col) points and higher clearing (Col-I) temperatures. This clearly indicates that the presence of three consecutive alkoxy tails in TSANs favors the Col assembly over wide thermal range; the effective space-filling and a greater core−core packing within a column may be the cause for such a behavior. The first member **TT-4** exhibits two enantiotropic Col phases, in contrast to the non-mesomorphic dialkoxy analogue, **DT-4**; this comparison, in part, supports our aforementioned assumption concerning the effective space-filling and a greater core−core packing. Upon cooling the sample **TT-4** slowly from the isotropic phase, a mesophase appears with a dendritic growth (Figure 3a) that quickly fills the field of view to furnish a mosaic pattern. The dendritic textural pattern suggests the mesophase

(22) (a) Destrade, C.; Foucher, P.; Gasparoux, H.; Nguyen, H. T.; Levelut, A. M.; Malthete, J. *Mol. Cryst. Liq. Cryst.* **1984**, *106*, 121−146. (b) Artal, M. C.; Toyne, K. J.; Goodby, J. W.; Barbera, J.; Photinos, D. J. *J. Mater. Chem.* **2001**, *11*, 2801−2807. (c) Alavarez, L.; Barbera, J.; Puig, L.; Romero, P.; Serrano, J. L.; Sierra, T. *J. Mater. Chem.* **2006**, *16*, 3768−3773.

(23) (a) Hayer, A.; de Halleux, V.; Kohler, A.; El-Garoughy, A.; Meijer, E. W.; Barbera, J.; Tant, J.; Levin, J.; Lehmann, M.; Gierschner, J.; Cornil, J.; Geerts, Y. H. *J. Phys. Chem. B.* **2006**, *110*, 7653−7659. (b) Barbera, J.; Gimenez, R.; Serrano, J. L. *Chem. Mater.* **2000**, *12*, 481−489 and references cited therein. (c) Carfagna, C.; Roviello, A.; Sirigu, A. *Mol. Cryst. Liq. Cryst.* **1985**, *122*, 151−160. (d) Gramsbergen, E. F.; Hoving, H. J.; de Jeu, W. H.; Praefcke, K.; Kohne, B. *Liq. Cryst.* **1986**, *1*, 397−400. (e) Metersdorf, H.; Ringsdorf, H. *Liq. Cryst.* **1989**, *5*, 1757−1772. (f) Zeng, H.; Carroll, P. J.; Swager, T. M. *Liq. Cryst.* **1993**, *14*, 1421−1429.

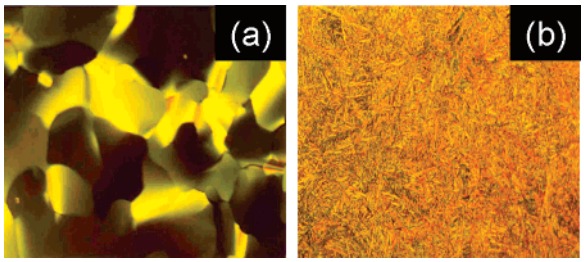

FIGURE 4. Photomicrographs of the optical textures obtained for the Col_h phase at 181 °C (a) and the Col_r phase at 156 °C (b) of compound **TT-8**.

TABLE 4. The Results of Indexation of XRD Profiles at a Given Temperature (*T*) of Col Phases Formed by the TSANS of the TT-*n* Series

compd	*T* (°C)	phase	*d* (Å) measd	*d* (Å) calcd	Miller index *hkl*	lattice parameters (Å)
TT-4	230	Col_h	20.5	20.5	100	$a = 23.6$
			11.8	11.8	110	$c = 3.42$
			10.3	10.2	200	
			7.8	7.7	210	
			6.7	5.9	220	
			4.4			
			3.42		001	
	190	Col_r	21.7	21.5	200	$a = 43.0$
			20.1	20.3	110	$b = 23.0$
			18.3	15.7	210	$c = 3.52$
			11.8	11.5	020	
			10.9	10.2	220	
			8.0	8.1	510	
			7.4	7.2	600	
			6.7	6.8	610	
			4.4			
			3.52		001	
TT-8	175	Col_h	24.5	24.5	100	$a = 28.3$
			14.1	14.2	110	$c = 3.54$
			12.2	12.3	200	
			9.3	9.3	210	
			6.7	7.1	220	
			4.5			
			3.54		001	
	150	Col_r	25.7	25.7	200	$a = 51.3$
			24.6	24.6	110	$b = 28.0$
			9.4	9.5	420	$c = 3.49$
			6.7	6.5	720	
			4.5			
			3.49		001	
TT-8B	90	Col_h	24.8	24.76	100	$a = 28.6$
			4.9			$c = 3.55$
			3.55		001	
	50	Col_r	25.4	25.4	200	$a = 47.3$
			23.7	23.7	110	$b = 30.2$
			4.9			$c = 3.57$
			3.57		001	

to be a Col phase. On further cooling, a transition to another Col phase occurs that was evident from the sharp change in the optical texture; tiny needles that grow on the mosaic texture of the higher temperature Col phase (Figure 3b) coalesce to yield a nonspecific texture. The transition temperature obtained was corroborated by the DSC measurements. The XRD data given in Table 4 confirm that the high- and low-temperature mesophases are Col_h and Col_r phases, respectively. The diffraction pattern obtained for the high-temperature Col phase consisted of a set of sharp reflections in the low-angle region besides two diffuse peaks at about 4.4 and 3.4 Å in the wide angles. The low-angle peaks are in the ratio of 1:0.58:0.5:0.38 which are indexed as (100), (110), (200), and (210) reflections of a 2D

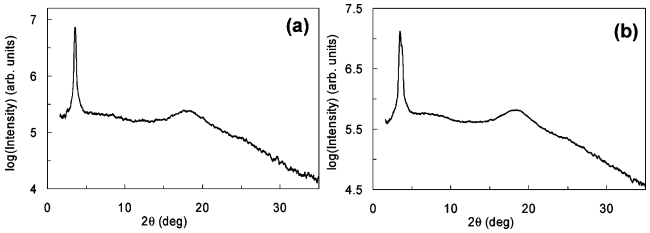

FIGURE 5. 1D intensity vs 2θ profiles obtained for the Col_h phase (a) and the Col_r phase (b) of the compound **TT-8B** at 90 and 50 °C, respectively.

hexagonal lattice with a spacing of about 24 Å. Figure 3c gives the 1D intensity vs the 2θ profile derived from the 2D pattern of the low-temperature Col phase. Notably, the low-angle region of the diffractogram comprises eight strong reflections, the maxima, which are best assigned to a rectangular columnar arrangement with cell parameters $a = 43$ Å and $b = 23$ Å. In addition to these, a diffuse peak with its center around 4.3 Å was observed in the wide-angle region, which is associated with the liquid-like correlation between aliphatic chains. The (001) reflection at about 3.5 Å indicates the periodic stacking of the molecular cores within the columns. Thus, XRD study suggests that the lower temperature mesophase of **TT-4** is the Col_r phase, although it displays an uncharacteristic optical texture.

The middle and higher homologues, viz., **TT-5** to **TT-8**, **TT-10**, **TT-12**, and **TT-16**, as mentioned earlier, show similar phase behavior; the occurrence of the dimesomorphic Col_r-Col_h sequence was identified for all these compounds by textural observation. As a representative case, the textural patterns of the Col_h and Col_r phases of **TT-8** are shown in Figure 4, parts a and b, respectively. The unequivocal assignment of the structures of these two mesophases of **TT-8**, again as a representative case, was achieved by the XRD studies and the results are summarized in Table 4. The XRD profile of the high-temperature phase showed five sharp reflections in the low-angle region.[16] The reciprocal spacings of these reflections have the ratio $1:\sqrt{3}:\sqrt{4}:\sqrt{7}:\sqrt{12}$, which could be indexed as (100), (110), (200), (210), and (220) reflections of a hexagonal lattice. Apart from these reflections, the diffractogram showed two broad reflections in the wide-angle region demonstrating that the ordering within the columns is not long-range. Similarly, the XRD pattern of the low-temperature mesophase showed two broad diffuse scatterings as well as four sharp Bragg reflections which could be, however, indexed to a rectangular 2D lattice of the Col phase. Thus, analysis of the results of these complementary studies indicates that TSANs comprising nine peripheral alkoxy chains stabilize hexagonal and rectangular Col phases in a dimesomorphic sequence. It is worth mentioning here that for compounds **TT-6** and **TT-7** the Col phase seems to freeze into a glassy state.

Compound **TT-8B** also displayed columnar behavior; unlike its dialkoxy analogue **DT-8B**, it showed two columnar phases which we describe as follows. On cooling from the isotropic phase, it showed a mesophase with a texture having fan-shaped defects and homeotropic digitated stars, which is typical of the Col_h phase.[16] On further cooling, a transition to another mesophase occurs via a textural change in which a transient needle pattern coalesces to a grainy texture. In this case also, the Col phase, especially the lower temperature phase, was found to be stable over a wide thermal range through room temperature. As summarized in Table 4, the analyses of the XRD patterns revealed that the high-temperature phase is Col_h with

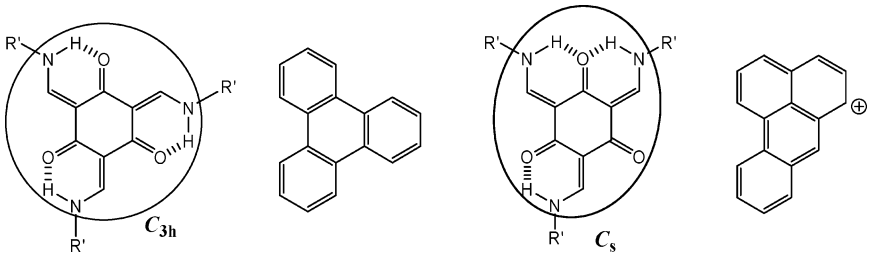

FIGURE 6. The C_{3h} and C_s geometrical forms of TSANs and their pseudostructural resemblance to the triphenylene and benz[*d*]anthracenylium systems, respectively.

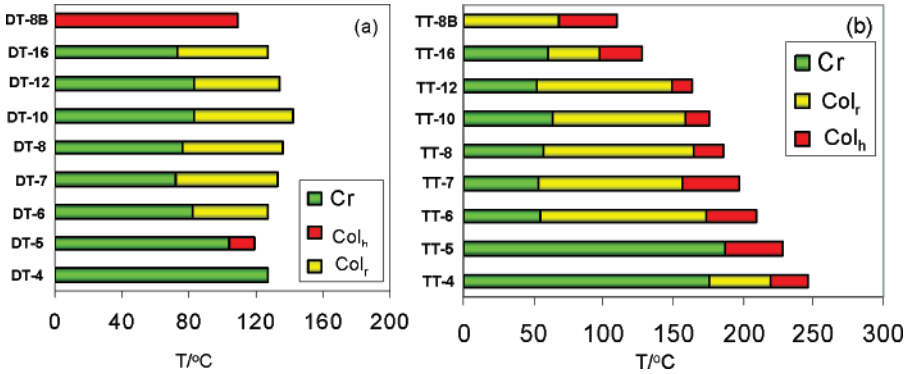

FIGURE 7. Graphical representation of the phase behavior (while heating) of the **DT-*n*** (a) and **TT-*n*** (b) series of TSANs.

the lattice constant $a = 28.6$ Å (Figure 5a) and the low-temperature phase is Col_r with the lattice constants $a = 47.3$ Å and $b = 30.2$ Å. (Figure 5b). The core−core separation peak was found to be centered around 3.6 Å.

Packing Within the Columns and Overview of the Phase Behavior. Tris(*N*-salicylideneaniline)s realized in the present study match the design concept of discotics; their C_{3h} and C_s tautomers form shape-persistent central rigid cores that are surrounded by flexible tails. The intrinsic intramolecular H-bonding among the H-atoms of the 2°-amine and carbonyl groups of the central cyclohexane-1,3,5-trione ring imposes shapes to the tautomeric forms. Importantly, depending upon the structures of the tautomers, the extent (number) of intramolecular H-bonding varies, and thus, their overall shapes differ. For example, in the C_{3h} isomer all the carbonyl groups are involved in H-bonding, and it bears a resemblance to the triphenylene (Figure 6); consequently it has been regarded as a *pseudo*-triphenylene.[13a] On the other hand, the C_s isomer resembles a four-ring noncircular aromatic core, the benz[*d*]-anthracenylium, if two of the three carbonyl groups of the central core are participating in the H-bonding. However, owing to the presence of peripheral alkoxy tails in the benz[*d*]anthracenylium-like structures, it may be reasonable to consider that the overall shape of the C_s isomer is disk-like. Eventually, the coassembly of both shape-persistent rotational isomers into columns and their further organization leads to the formation of a fluid macroscopic structure having a 2D lattice of different symmetries. Furthermore, it is apparent that the extent of Col mesomorphism of TSANs is susceptible to the nature and the number of alkoxy chains at the exterior position: TSANs with two alkoxy tails on each of the three exterior benzene rings linked to the central cyclohexanetrione core exhibit Col_h or Col_r phases, while their trialkoxy analogues stabilize a dimesomorphic sequence involving a transition from hexagonal to rectangular Col phases. The majority of TSANs having three exterior alkoxy chains show lower melting (Cr-Col) points and higher

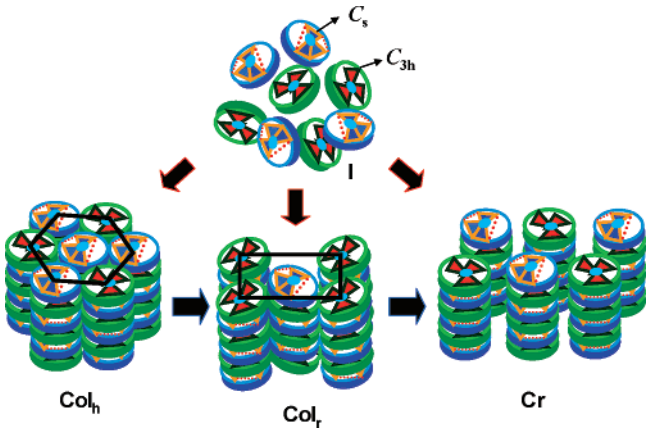

FIGURE 8. Schematic representation of the self-organization of C_{3h} and C_s tautomers of TSANs into phase(s) during cooling from their isotropic liquid state.

clearing (Col-I) temperatures when compared with those of dialkoxy compounds. The effective space-filling and a greater core−core packing within a column of trialkoxy derivatives may be the reason for their above-mentioned behavior. The graphical representations of phase behavior and thus the thermal range of the mesophases of **DT-*n*** and **TT-*n*** series are given in Figure 7, parts a and b, respectively. The general phase behavior of the TSANs has been schematically shown in Figure 8.

Optical Absorption and Fluorescence Behavior. As discussed before, owing to the presence of multiple chromophores and possible π-conjugations between the peripheral region and the central core, both series of discotics TSANs are expected to exhibit promising photophysical properties. Thus, UV−vis absorption and fluorescence characteristics of some of the representative compounds randomly selected from both the series, viz., **DT-8**, **TT-8**, and **TT-8B**, were studied in solution as well as in the mesophase. Indeed, the THF solution absorption

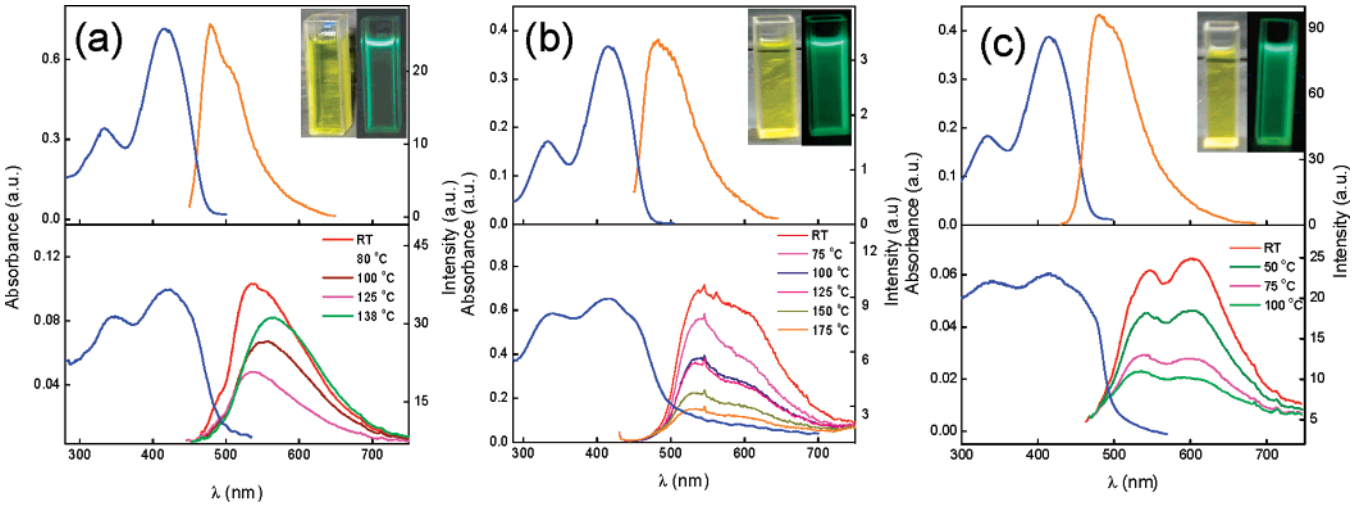

FIGURE 9. Absorption and emission spectra in THF solution (top panels) and in the thin films of the mesophases (lower panels) obtained for **DT-8** (a), **TT-8** (b), and **TT-8B** (c). The inset shows the pictures of solutions as seen before (LHS) and after the illumination (RHS) of light of 365 nm. Note that for thin films of the Col phase, the spectra were recorded as a function of temperature (see RHS traces of lower panels) (LHS = left-hand side; RHS = right-hand side.)

TABLE 5. Photophysical Properties of TSANS DT-8, TT-8, and TT-8B

	THF solution[a]			glassy film		
$TSAN_s$	absorption[b]	emission[b,c]	Stokes shift	absorption[b]	emission[b,c]	Stokes shift
DT-8	334, 416	481	65	341, 424	539	123
TT-8	334, 416	484	65	339, 418	545,612	138
TT-8B	332, 416	480	64	336, 414	531, 616	202

[a] Micromolar solutions in THF. [b] Wavelengths (nm). [c] The excitation wavelength λ_{ex} = 416 nm.

spectra were recorded for all the compounds and their pattern looked alike, as expected. As shown in the upper and lower panels of Figure 9a−c, UV−vis spectra (blue trace) of the three investigated TSANs in solution and mesophase respectively showed two absorption maxima centered around 335 and 416 nm corresponding to $\pi-\pi^*$ and $n-\pi^*$ transitions. Upon irradiating these solutions with one of the absorption maxima, viz., 416 nm, a fluorescence maximum was observed at around 482 nm with a negligible shoulder (orange traces in the upper panels of Figure 9a−c). The Stokes shift, which is the difference between the spectral positions of the band maxima of the absorption and fluorescence arising from the same electronic transition, was found to be in the range of 64−65 nm (Table 5). The occurrence of luminescence at a longer wavelength than the absorption is in agreement with the general observation. As shown in the insets, the green light is visually perceivable in the emissive state.

The absorption behavior of the fluid Col phase as well as its frozen state in the form of a thin film were investigated. The sample under investigation was held between the two cover slips and cooled slowly (1 deg/min) from the isotropic liquid state until room temperature. To begin with, the emission spectra were recorded at room temperature. As already mentioned above, the frozen Col structures of **DT-8** and **TT-8** and the room-temperature Col phase of **TT-8B** show two absorption bands analogous to those in the solution state. The apparent small red shift in the two absorption maxima of the Col structure is indicative of the intimate overlap of the fluorophores in such states. When excited at 416 nm, two broad bands with fluorescence maxima are observed at around 530 and 600 nm for compounds **TT-8** and **TT-8B** (see red traces of the lower panels b and c of Figure 9), while for TSAN **DT-8** only a fluorescence maximum at around 539 nm was obtained. The fluorescence spectra of these thin films at different temperatures starting from the room temperature/glassy Col phase for the above-mentioned excitation wavelength were measured and have been shown in the right-hand side of the lower panels a−c of Figure 9. As can be seen, the intensity of the emission peak decreases progressively with the increase in the temperature that can be attributed to breaking of larger columnar stacks into smaller ones and thermally activated radiationless processes.[24] Notably, when compared with the emission behavior of solution, the films of the neat Col phase exhibit a strong bathochromic (red) shift that can be attributed to the strong co-facial proximity of C_{3h} and C_s isomers within the Col structure as well as the formation of excimers/aggregates. Generally, the excimers are regarded as molecular dimers or a stoichiometric complex with associated excited electronic states, dissociative ground states, and structureless emission spectra.[25] Furthermore, the spectral pattern with two emission maxima of the trialkoxy compounds **TT-8** and **TT-8B** as compared to only a broad fluorescence maximum of dialkoxy TSAN **DT-8** perhaps reflects on the dissimilar arrangement of the discs with six or nine peripheral alkoxy tails within the columns; however, it must be mentioned here that it is rather difficult to comment on the precise nature of the associated forms. Thus, it is apparent that the TSANs realized in the present investigation are capable of generating the light in both solution and mesophase states. This is especially

(24) (a) Kleppinger, R.; Lillya, C. P.; Yang, C. *J. Am. Chem. Soc.* **1997**, *119*, 4097−4102. (b) Festag, R.; Kleppinger, R.; Soliman, M.; Wendorff, J. H.; Lattermann, G.; Staufer, G. *Liq. Cryst.* **1992**, *11*, 699−710.

(25) (a) Birks, J. B. The Photophysics of Aromatic Excimers. In *The Exiplex*; Gordon, M., Ware, W. R., Eds.; Academic Press: New York, 1975; p 39. (b) Duan, X. F.; Wang, J.-L.; Pei, J. *Org. Lett.* **2005**, *19*, 4071−4074.

remarkable in the later situation wherein the 2D order with short intra-core distance facilitates motion of charges with impounding motion of the ionic impurities.[8b] Nonetheless, detailed investigations involving the annealing of films, film morphology, fluorescence efficiency, solvent effects, etc. are required to further elucidate the photophysical properties of TSANs quantitatively.

Summary. The synthesis and phase behavior of a novel class of discogens composed of TSANs are described. The principle objective of this investigation was to validate our recent demonstration that with the space-filling design concept, TSANs can be enforced to display columnar mesomorphism wherein the individual columns are built by the co-facial self-assembly of two shape-persistent rotational isomers formed of intramolecular H-bonding. Thus, several discotic TSANs belonging to two series each consisting of six and nine peripheral *n*-alkoxy/branched tails have been accomplished. In each series, the length of the *n*-alkoxy tail has been varied to learn about the correlation between structure and property. Our study using a combination of optical polarizing microscope, differential scanning calorimeter, and X-ray diffraction revealed that the mesomorphic behavior is sensitive to the number of exterior *n*-alkoxy tails rather than the length. Notably, several of them with *n*-alkoxy tails form a glassy Col structure in which the core−core separation is quite small. Of special significance, TSANs comprising branched alkoxy tails display the Col phase over a broad thermal range through room temperature. The absorption and fluorescence properties have been studied in the Col phase and in solution. The observed light emissive characteristic of the Col phase appears to be promising from the point of electronic device application given the fact that in such structures the proton and electron interact with each other through the H-bonding environment. In essence, owing to the ease of synthesis, structural diversity, columnar behavior, and electronic properties, discotic TSANs may find a place in electronic device application.

Experimental Section

General. For general experimental details and instrumentation, see the Supporting Information. The mesogenic compounds were investigated for their liquid crystalline behavior employing an optical polarizing microscope equipped with a programmable hot stage and differential scanning calorimeter. X-ray diffraction studies were carried on powder samples in Lindemann capillaries with Cu Kα radiation, using an Image Plate Detector equipped with a double mirror focusing optics. UV−vis spectra were recorded for solution and mesophase states. The above-mentioned optical polarizing microscope equipped with a programmable hot stage and differential scanning calorimeter was used to determine the melting points of non-mesomorphic compounds. Fluorescence emission spectra in solution and mesophase state were recorded with luminescence spectrometers.

All the 3,4-dialkoxynitrobenzenes (**3a**−**h**) and 3,4,5-trialkoxynitrobenzenes (**4a**−**h**) and the corresponding anilines **5a**−**h** and **6a**−**h** were prepared following the experimental procedure described below for the syntheses of **3b**, **4b**, **5b**, and **6b** as representative cases.

3,4-Dipentyloxynitrobenzene (3b). To an ice-cooled solution of 1,2-dipentyloxybenzene (**1b**) (2.5 g, 10 mmol, 1 equiv) in dichloromethane (15 mL) was added $NaNO_2$ (0.1 g, 1.4 mmol, 0.14 equiv) with stirring. To this ice-cooled suspension was added a solution of 70% HNO_3 (1.4 mL, 30 mmol, 3 equiv) in dichloromethane (12 mL); this mixture was allowed to attain room temperature and stirring was continued for 1 h. The reaction mass was poured into water and extracted with dichloromethane (4 × 100 mL). The combined extracts were washed with 5% aqueous $NaHCO_3$ solution, water, and brine then dried over anhyd Na_2SO_4 and concentrated. The crude product obtained was purified by column chromatography on silica gel (60−120 mesh). Elution with hexanes followed by 10% dichloromethane−hexanes yielded **3b**, which was further purified by recrystallization from ethanol. R_f 0.51 (30% CH_2Cl_2−hexanes); white solid; mp 50−52 °C; yield 1.6 g, 54%; IR (KBr pellet) ν_{max} in cm^{-1} 3020, 2960, 2875, 1517, 1340, 1217, 778, and 669; ^1H NMR ($CDCl_3$, 200 MHz) δ 7.87 (dd, 1H, J = 9.0 Hz, 2.6 Hz, Ar), 7.72 (d, 1H, J = 2.6 Hz, Ar), 6.88 (d, 1H, J = 9.0 Hz, Ar), 4.07 (q, 4H, J = 6.2 Hz, 2 × OCH_2), 1.27−1.92 (m, 12H, 6 × CH_2), 0.99 (t, 6H, J = 7.4 Hz, 2 × CH_3); MS (FAB^+) m/z for $C_{16}H_{25}NO_4$, calcd 295.2, found 295.9. Anal. Calcd for $C_{16}H_{25}NO_4$: C, 65.06; H, 8.53, N, 4.74. Found: C, 65.3; H, 8.8; N, 4.4.

3,4-Dipentyloxyaniline (5b). To a solution of nitro compound **3b** (2.95 g, 10 mmol, 1 equiv) in dry THF (20 mL) was added 10% Pd−C (0.3 g) with stirring under hydrogen atmosphere (balloon) for 12 h (monitored by TLC). The reaction mixture was filtered through a celite bed. Evaporation of the solvent yielded the amine that was passed through a very short basic alumina column, using a mixture of ethylacetate−hexanes (10%) as the eluent. The evaporation of solvent yielded pure amine **5b** as a viscous liquid; R_f 0.53 (30% EtOAc−hexanes); yield 2.4 g, 90%; IR (KBr pellet) ν_{max} in cm^{-1} 3360, 2931, 2869, 1512, 1468, 1227, 1180, 896, 748, and 599; ^1H NMR ($CDCl_3$, 200 MHz) δ 6.73 (d, 1H, J = 8.4 Hz, Ar), 6.30 (d, 1H, J = 2.4 Hz, Ar), 6.21 (dd, 1H, J = 8.4 Hz, 2.4 Hz, Ar), 3.92 (q, 4H, J = 6.8 Hz, 2 × OCH_2), 3.43 (br s, 2H, NH_2), 1.35 −1.87 (m, 12H, 6 × CH_2), 0.89 (t, 6H, J = 6.0 Hz, 2 × CH_3); MS (FAB^+) m/z for $C_{16}H_{27}NO_2$, calcd 265.2, found 265.9. Anal. Calcd for $C_{16}H_{27}NO_2$: C, 72.41; H, 10.25; N, 5.28. Found: C, 72.4; H, 10.3; N, 5.3.

3,4,5-Tripentyloxynitrobenzene (4b). The experimental procedure was as described for the preparation of **3b**. Quantities: **2b** (3.2 g, 9.5 mmol, 1 equiv), sodium nitrite (0.09 g, 1.3 mmol, 0.14 equiv), and 70% HNO_3 (1.3 mL, 28.5 mmol, 3 equiv). R_f 0.52 (30% CH_2Cl_2−hexanes); a pale yellow liquid; yield 2.18 g, 60%; IR (KBr pellet) ν_{max} in cm^{-1} 2956, 2934, 2872, 1617, 1524, 1493, 1467, 1390, 1339, 1234, 1115, 852, 794, 682, and 668; ^1H NMR ($CDCl_3$, 200 MHz) δ 7.47 (s, 2H, Ar), 4−4.1 (m, 6H, 3 × OCH_2), 0.91−1.88 (m, 27H, 9 × CH_2, 3 × CH_3); MS (FAB^+) m/z for $C_{21}H_{35}NO_5$, calcd 381.3, found 381.9. Anal. Calcd for $C_{21}H_{35}NO_5$: C, 66.11; H, 9.25; N, 3.67. Found: C, 66.5; H, 9.4; N, 3.9.

3,4,5-Tripentyloxyaniline (6b). The experimental procedure was as described for the preparation of **5b**. Quantities: **4b** (3.8 g, 10 mmol, 1 equiv), 10% Pd−C (0.38 g, 10% weight of the starting material), dry THF (15 mL). R_f 0.44 (30% EtOAc−hexanes); gray solid; mp 81−83 °C; yield 3.08 g, 88%; IR (KBr pellet) ν_{max} in cm^{-1} 3331, 2956, 2933, 1600, 1504, 1456, 1230, 1108, 1050, 756, and 585; ^1H NMR ($CDCl_3$, 200 MHz) δ 5.91 (s, 2H, Ar), 3.81−3.94 (m, 6H, 3 × OCH_2), 3.5 (br s, 2H, NH_2), 1.28−1.82 (m, 18H, 9 × CH_2), 0.92 (t, 9H, J = 6.4 Hz, 3 CH_3); MS (FAB^+) m/z for $C_{21}H_{37}NO_3$, calcd 351.3, found 351.8. Anal. Calcd for $C_{21}H_{37}NO_3$: C, 71.75; H, 10.61; N, 3.98. Found: C, 71.6; H, 10.5; N, 4.3.

All the target dialkoxy TSANs (**DT-*n*** series) and trialkoxy TSANs (**TT-*n*** series) were prepared following the experimental procedure described below for the synthesis of **DT-5** and **TT-5** as representative cases.

(2*E*,4*E*,6*E*)-2,4,6-Tris((3,4-dipentyloxyphenylamino)methylene)cyclohexane-1,3,5-trione (C_{3h} isomer) and (*Z*)-2,4,6-Tris((3,4-dipentyloxyphenylamino)methylene)cyclohexane-1,3,5-trione (C_s isomer) (DT-5). A mixture of triformylphloroglucinol (0.084 g, 0.4 mmol, 1 equiv) and compound **5b** (0.72 g, 2.7 mmol, 6.75 equiv) in absolute ethanol (15 mL) was heated to reflux under an inert atmosphere for 2 h with vigorous stirring. The pale yellow solid separated upon cooling the reaction mixture was collected by filtration, repeatedly washed with ethanol, and air-dried. The crude product **DT-5** was further purified by repeated recrystalli-

zations in a mixture of absolute ethanol−dichloromethane (9:1). R_f 0.54 (30% EtOAc−hexanes); a yellow solid; yield 0.29 g, 75%; UV−vis: λ_{max} = 415.97 nm, $\epsilon = 5.4792 \times 10^4$ L mol^{-1} cm^{-1}; IR (KBr pellet) ν_{max} in cm^{-1} 3450, 2930, 2859, 1621, 1591, 1522, 1459, 1262, 1136, 988, and 820; ^{1}H NMR ($CDCl_3$, 400 MHz) δ 13.47 (d, J = 13.0 Hz, ═CNH), 13.36 (d, J = 13.2 Hz, ═CNH), 13.01(d, J = 13.2 Hz, ═CNH), 12.97 (d, J = 13.2 Hz, ═CNH) (these four resonances are due to 3H), 8.63−8.8 (m, 3H, ═CHN), 6.81−6.91 (m, 9H, Ar), 3.98−4.10 (m, 12H, 6 × OCH_2), 0.92−1.85 (m, 54H, 18 × CH_2, 6 × CH_3); MS (FAB^+) m/z for $C_{57}H_{82}N_3O_9$ (M + 1), calcd 952.6, found 952.8; Anal. Calcd for $C_{57}H_{81}N_3O_9$: C, 71.89; H, 8.57; N, 4.41. Found: C, 71.5; H, 8.7; N, 4.4.

(2*E*,4*E*,6*E*)-2,4,6-tris((3,4-Trialkyloxyphenylamino)methylene)-cyclohexane-1,3,5-trione (C_{3h} isomer) and (*Z*)-2,4,6-Tris((3,4-trialkyloxyphenylamino)methylene)cyclohexane-1,3,5-trione (C_s isomer) TT-5. The experimental procedure was as described for the preparation of **DT-5**. Quantities: triformylphloroglucinol (0.084 g, 0.4 mmol, 1 equiv), **6b** (0.95 g, 2.7 mmol, 6.75 equiv), and absolute ethanol (15 mL). The pale yellow solid separated upon cooling the reaction mixture was collected by filtration, repeatedly washed with ethanol, and air-dried. The crude product **TT-5** was further purified by repeated recrystallizations in a mixture of absolute ethanol−dichloromethane (9:1). R_f 0.59 (30% EtOAc−hexanes); a yellow solid, yield 0.39 g, 80%; UV−vis: λ_{max} = 415.06 nm, $\epsilon = 7.3046 \times 10^4$ L mol^{-1} cm^{-1}; IR (KBr pellet) ν_{max} in cm^{-1} 3452, 2956, 2871, 1622, 1588, 1508, 1459, 1289, 1230, 1113, 987, and 824; ^{1}H NMR ($CDCl_3$, 400 MHz) δ 13.46 (d, J = 13 Hz, ═CNH), 13.28 (d, J = 13.2 Hz, ═CNH), 13.01 (d, J = 13.2 Hz, ═CNH), 12.88 (d, J = 13.4 Hz, ═CNH) (these four resonances are due to 3H), 8.62−8.78 (m, 3H, ═CHN), 6.48 (s, 6H, Ar), 3.92−4.03 (m, 18H, 9 × OCH_2), 0.92−1.85 (m, 81H, 27 × CH_2, 9 × CH_3); MS (FAB^+) m/z for $C_{72}H_{113}N_3O_{12}$ (M + 2), calcd 1211.8, found 1212.5. Anal. Calcd for $C_{72}H_{111}N_3O_{12}$: C, 71.43; H, 9.24; N, 3.47. Found: C, 71.2; H, 9.4; N, 3.6.

Supporting Information Available: General experimental details, instrumentation, structural characterization data, ^{1}H NMR spectra of all the target molecules and representative intermediates (**1e**, **3e**, **5e**, **2e**, **4e**, and **6e**), ^{1}H−^{1}H COSY NMR spectra of **DT-8**, **TT-8**, and **TT-8B**, ^{13}C NMR of **DT-8** and **TT-8**, photomicrographs of the optical textures of **DT-5** and **TT-8B**, DSC traces of **DT-8**, **TT-8**, and **TT-8B**, and XRD patterns of **DT-5**, **DT-8**, and **TT-8**. This material is available free of charge via the Internet at http://pubs.acs.org.

JO0712650